Supplement of Atmos. Chem. Phys., 24, 8751–8770, 2024
https://doi.org/10.5194/acp-24-8751-2024-supplement

Atmospheric Chemistry and Physics
Open Access

Supplement of

Vertically resolved aerosol variability at the Amazon Tall Tower Observatory under wet-season conditions

Marco A. Franco et al.

Correspondence to: Marco A. Franco (marco.franco@usp.br) and Christopher Pöhlker (c.pohlker@mpic.de)

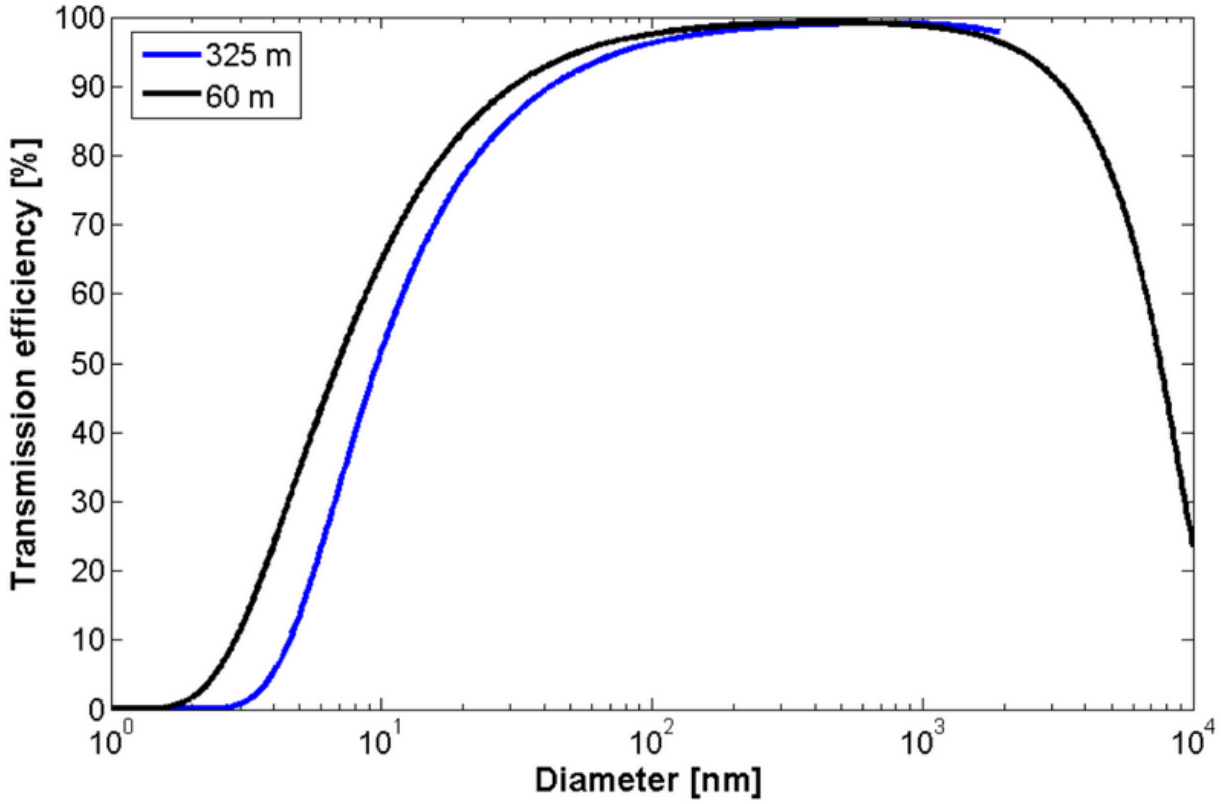

Figure S1. Transmission efficiency curves obtained using the Particle Loss Calculator software, similarly to Holanda et al. (2023) for the 60 (black) and 325 m (blue) inlet lines.

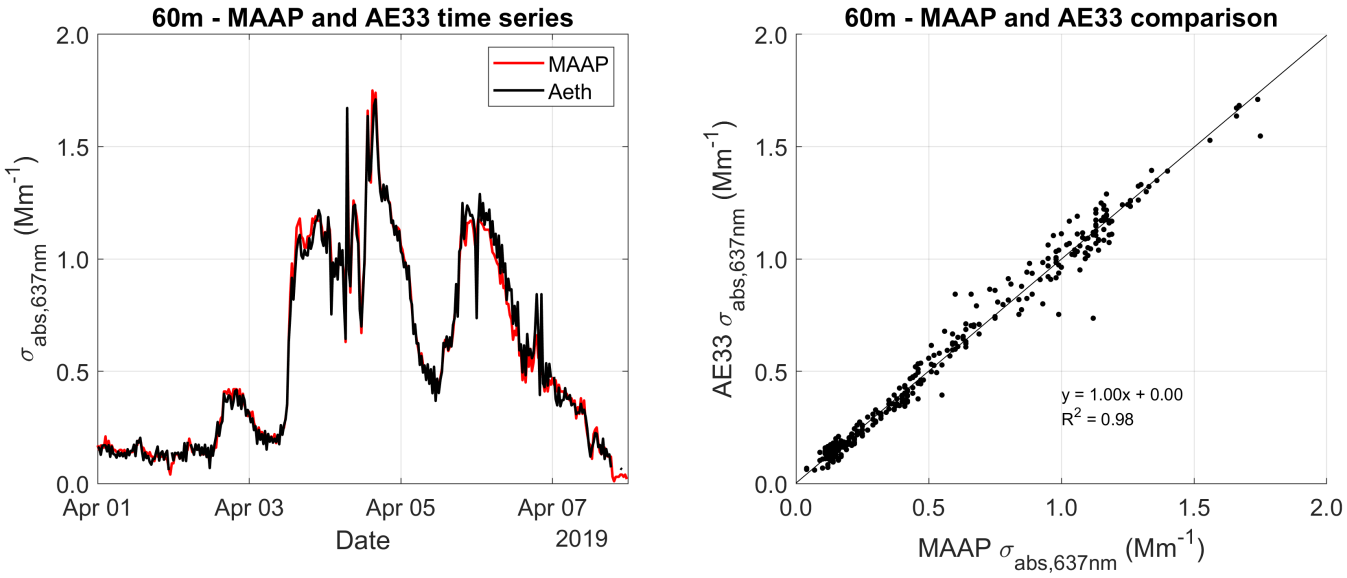

Figure S2. Comparison between the absorption coefficients measured by the MAAP and the AE33 at 60 m for April 01-08, 2019. On the left is the time series of both instruments and on the right is the correlation plot.

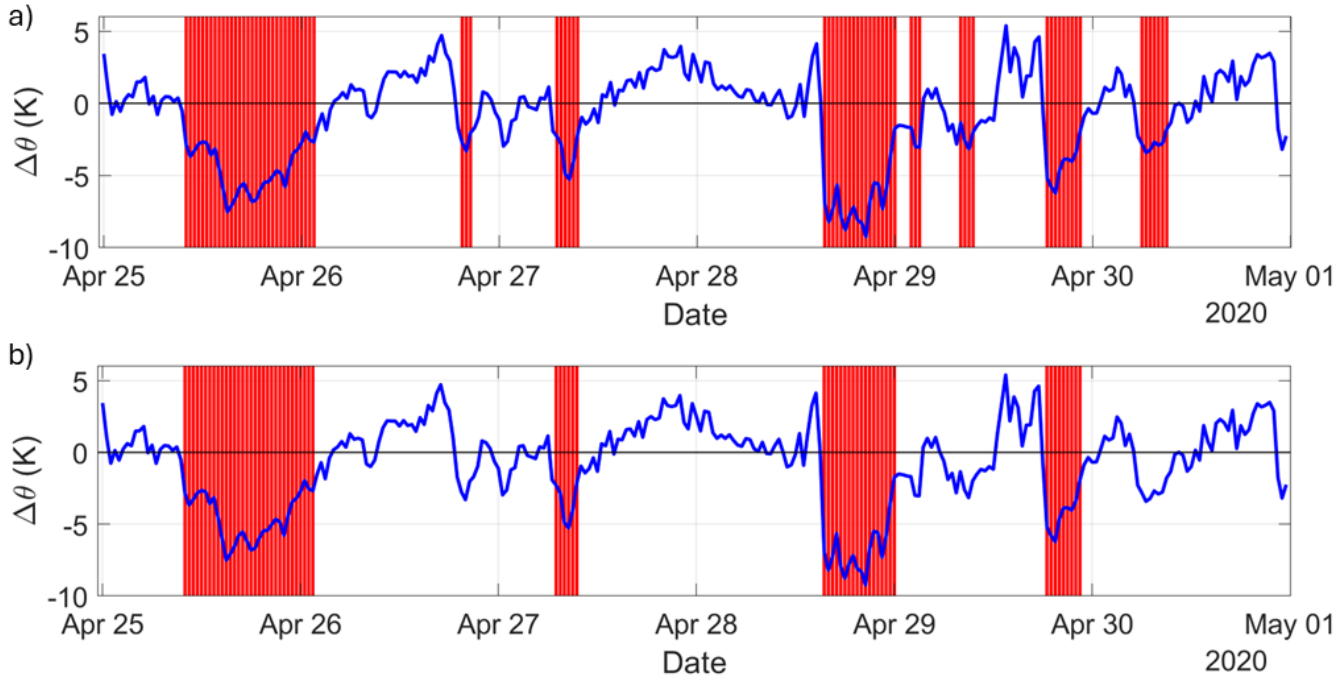

Figure S3. Examples of the algorithm application for downdraft detection, applied to 25-30 April 2020. All events are considered in plot (a), and in the plot (b), only the most intense events selected above the established threshold are detected. In both windows, the blue curve represents the time series of the potential temperature anomaly, and the red-shaded areas indicate the periods the algorithm considered belonging to a convective event. The horizontal black line indicates $\Delta\theta = 0$.

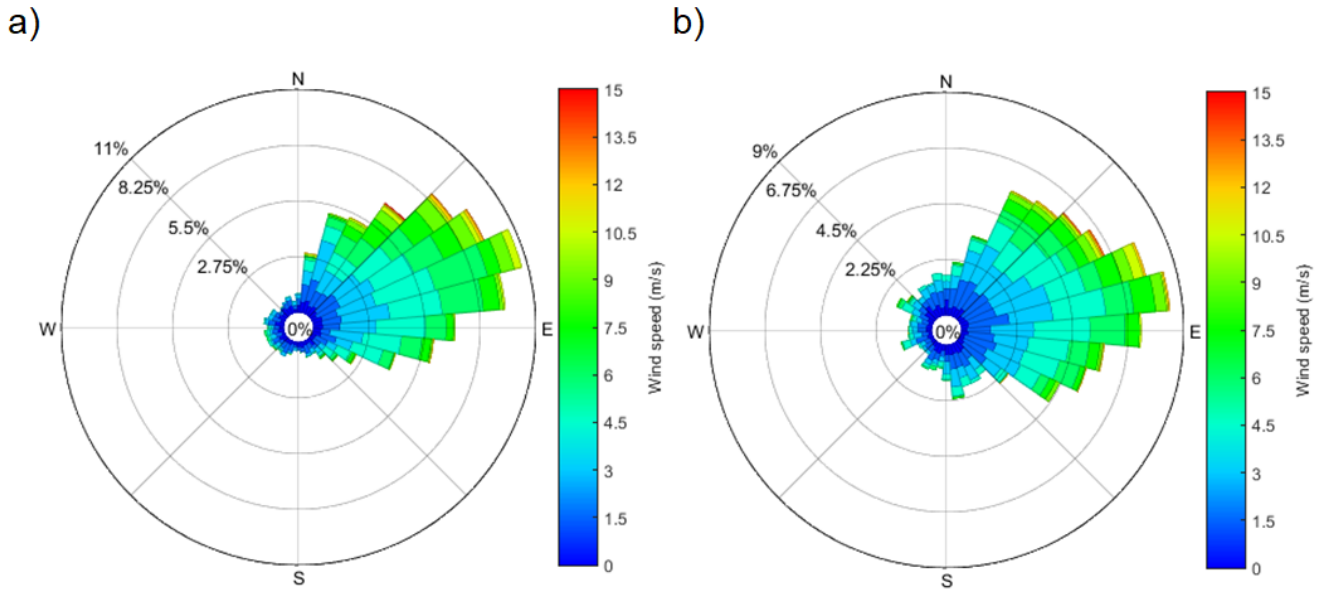

Figure S4. The wind rose for April and May a) 2019 and b) 2020. The color bar expresses the wind speed ($\mathrm{m\ s^{-1}}$), and the percentages in the figure represent the data coverage.

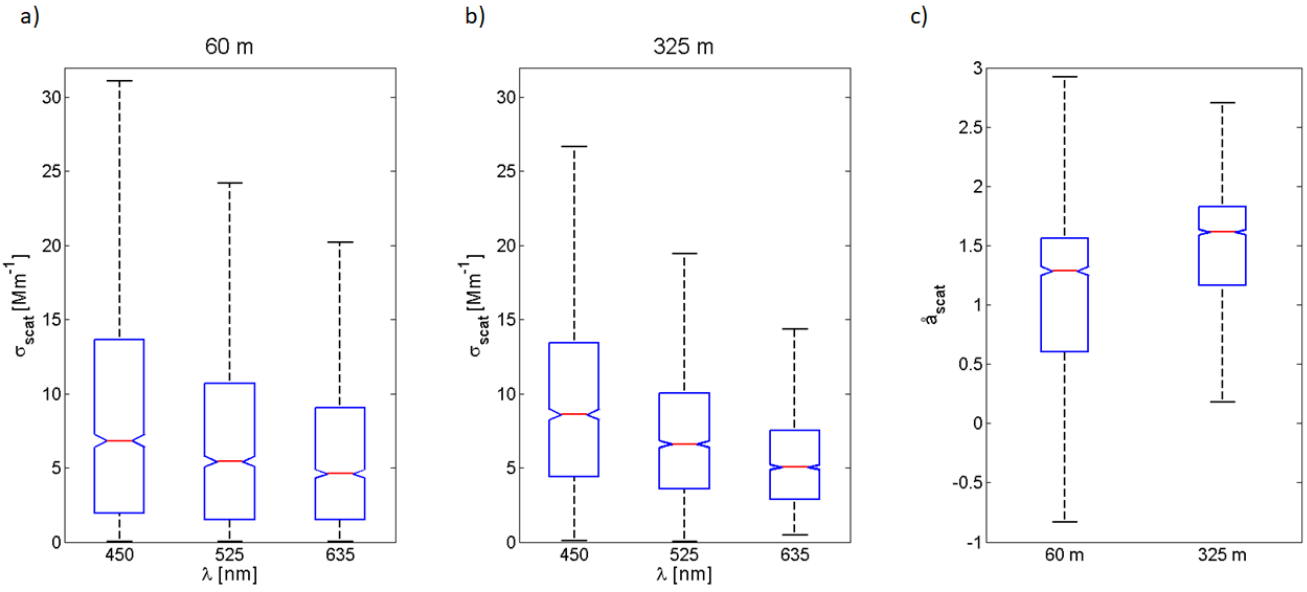

Figure S5. Comparative boxplots of aerosol scattering coefficients at wavelengths 450, 525, and 635 nm at a) 60 m and b) 325 m. In c), the comparative boxplot of the mean scattering Ångström exponent is presented. The box represents the quartiles, the whiskers represent the 90th and 10th percentiles, and the horizontal line represents the median.

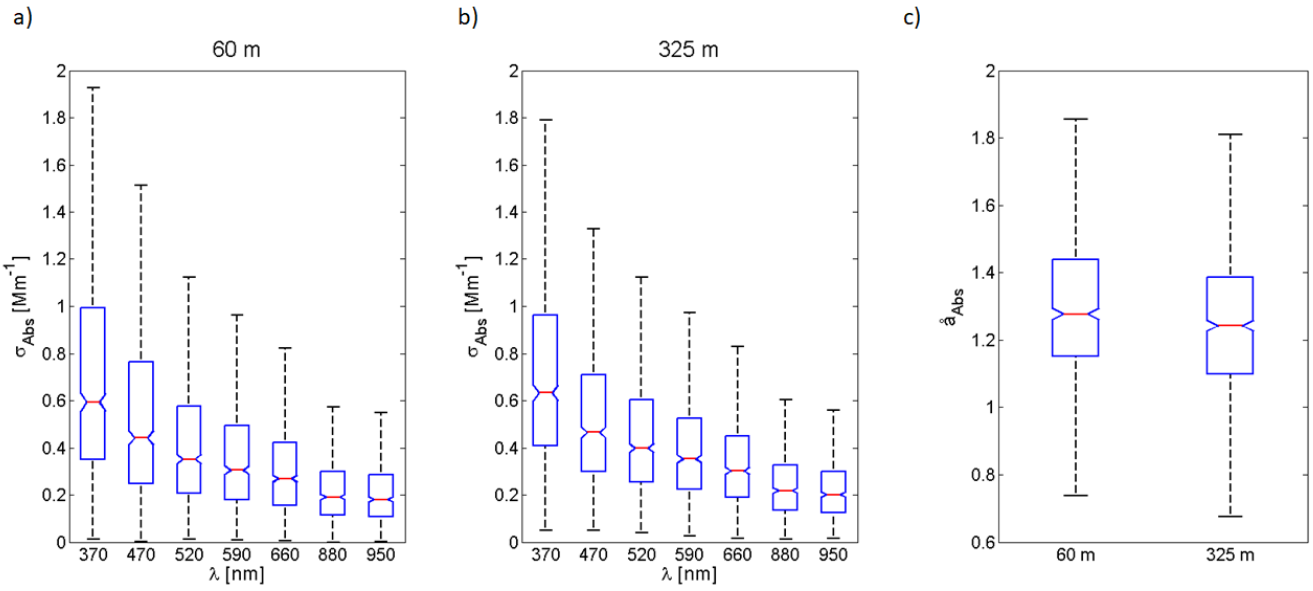

Figure S6. Comparative boxplots of aerosol absorption coefficients at $\lambda = 370$, 470, 520, 590, 660, 880 and 950 nm at a) 60 and b) 325 m height. In c), the comparative boxplot of the mean absorption Ångström exponent is presented. The box represents the quartiles, the whiskers represent the 90th and 10th percentiles, and the horizontal line represents the median.

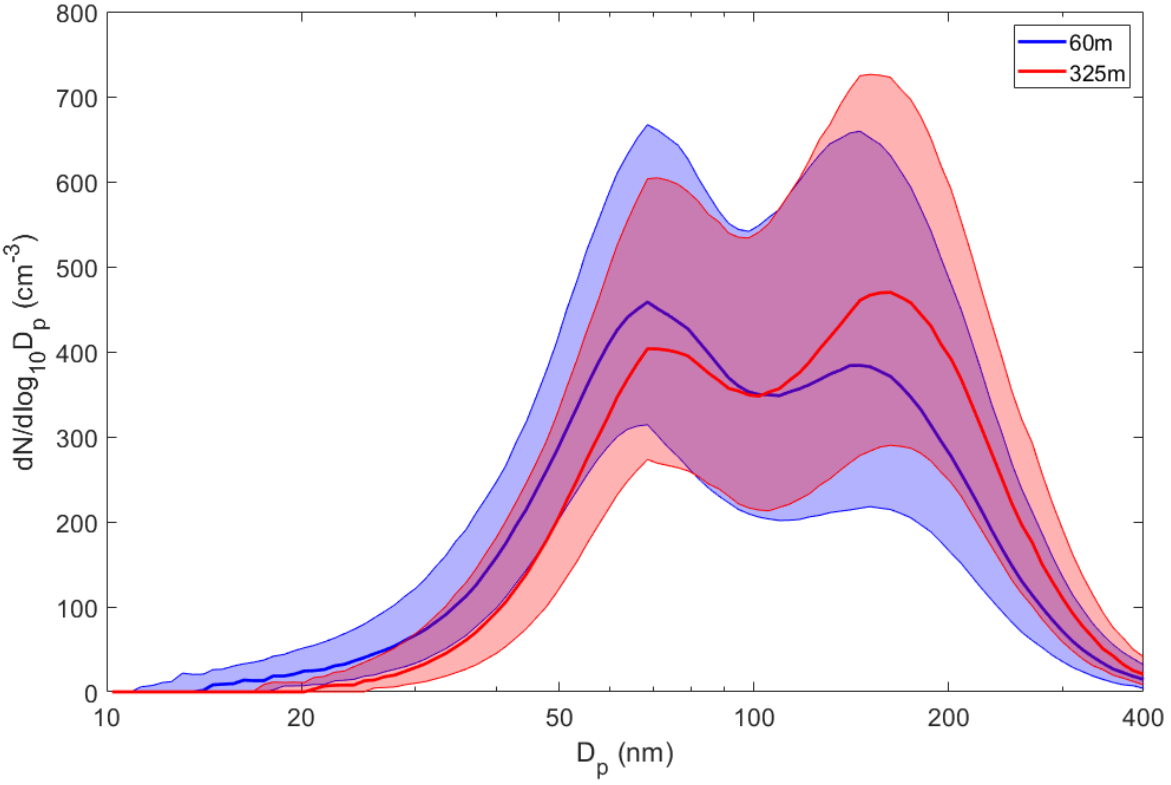

Figure S7. Median aerosol size distributions in the vertical profile. The blue line is the median aerosol size distribution at 60 m high, and the green line is the median aerosol size distribution at 325 m high. Colored shaded areas indicate the interquartile ranges.

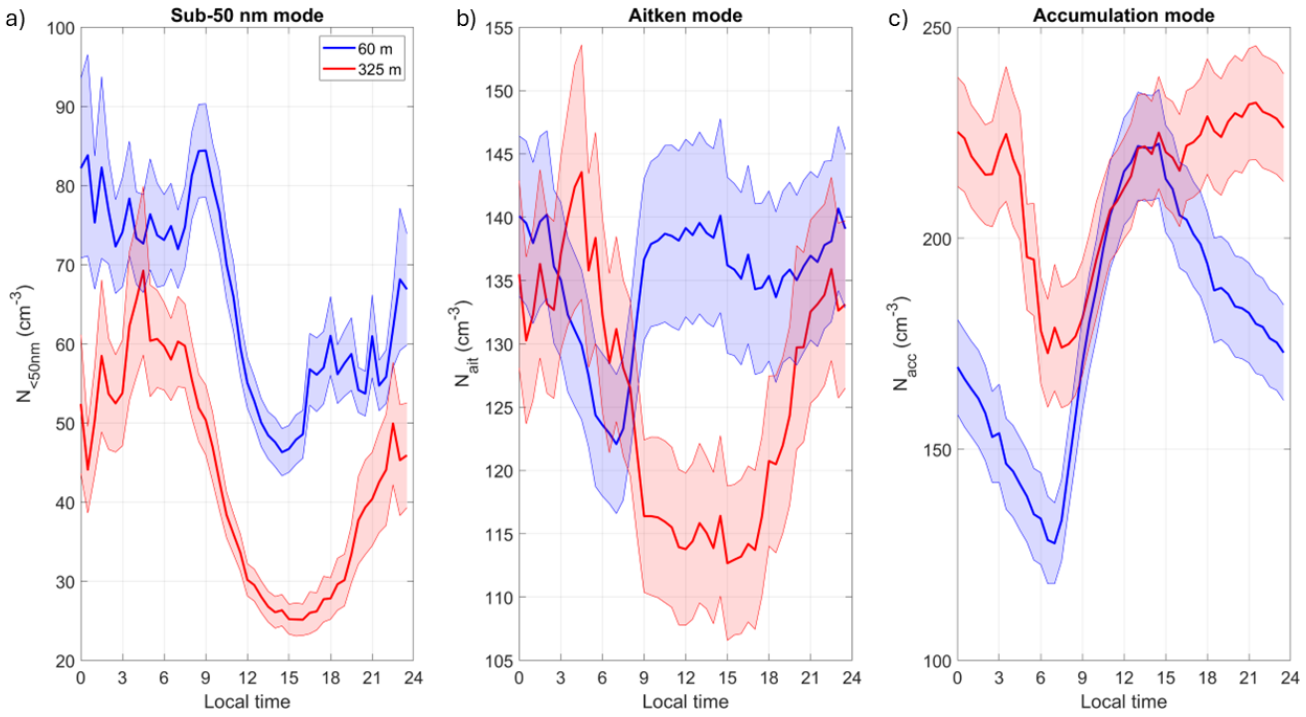

Figure S8. Mean diurnal cycle of particle number concentrations in the a) sub-50 nm, b) Aitken, and c) accumulation modes. Bars are the standard error.

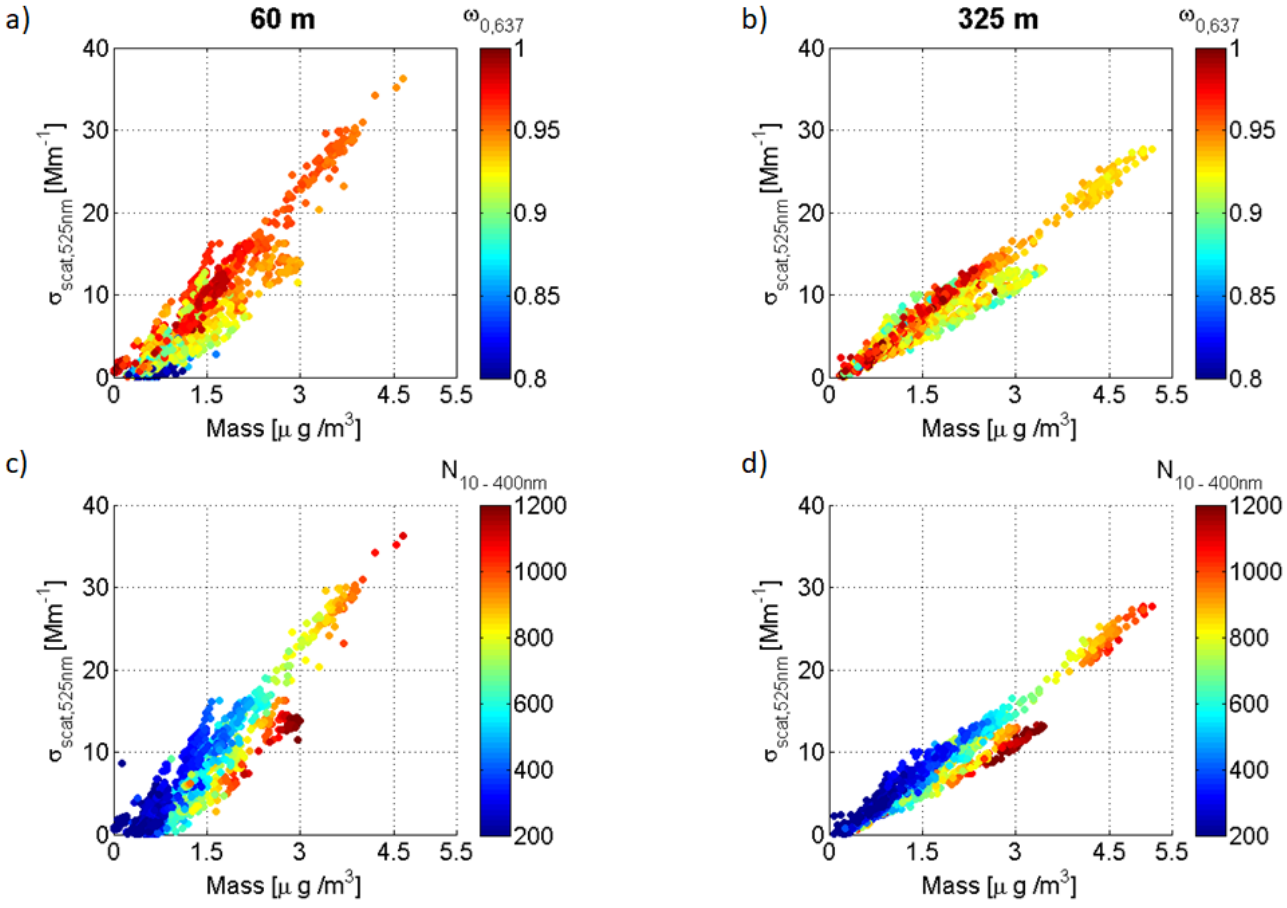

Figure S9. Scattering coefficient, $\sigma_{scat,525nm}$, as a function of the mass concentration for measurements at 60 and 325 m height. The colors in panels a) and b) represent $\omega_{0,637nm}$, and the colors in c) and d) represent $N_{10-400nm}$. The mass concentration is obtained by multiplying the aerosol volume (in size range 10 to 400 nm) by the average mass loading of the wet season (1.4 µg m^{-3}) (Artaxo et al., 2022)

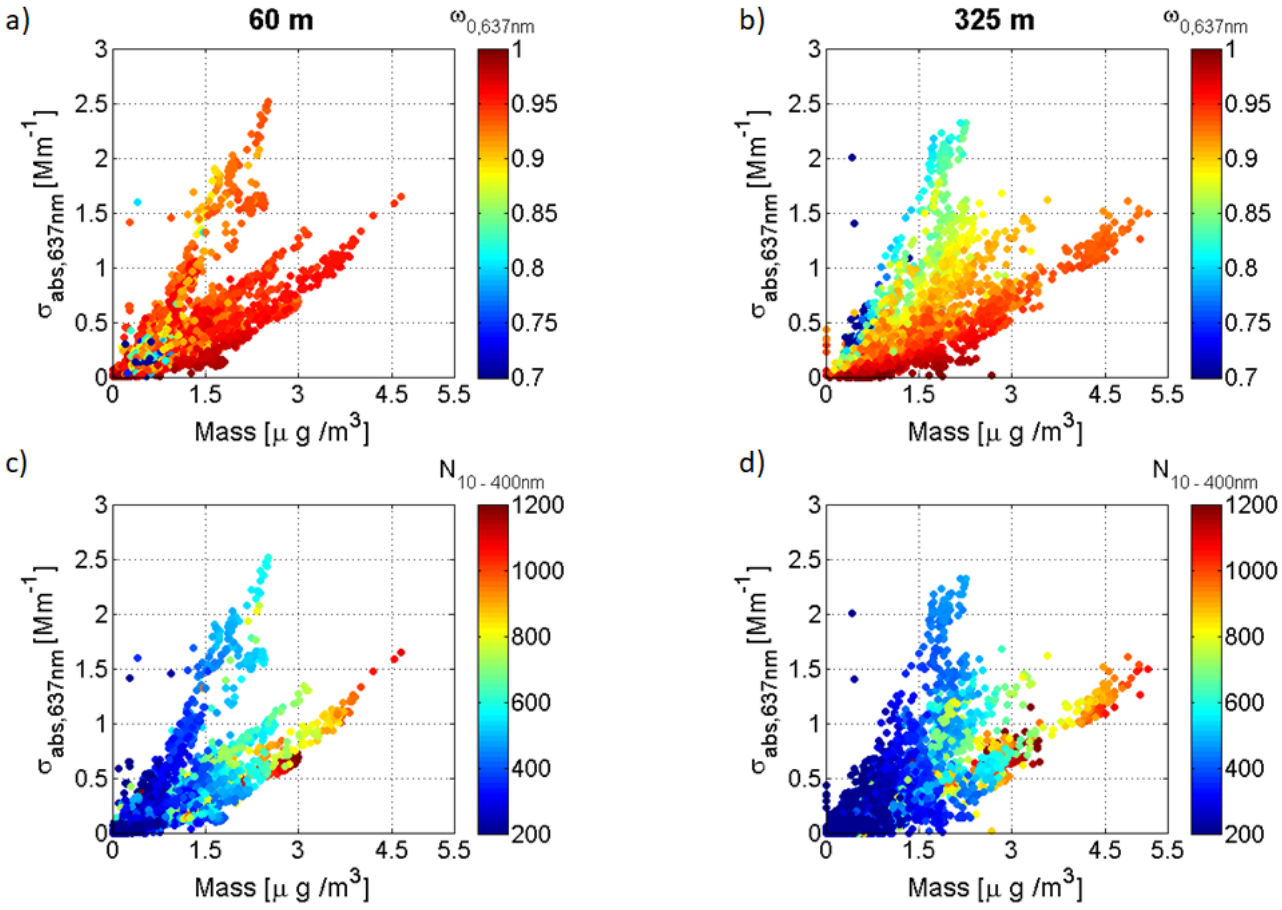

Figure S10. Absorption coefficient, $\sigma_{abs,637nm}$, as a function of mass concentration for measurements at 60 and 325 m height. The colors in panels a) and b) represent $\omega_{0,637nm}$, and the colors in c) and d) represent $N_{10-400nm}$. The mass concentration is calculated by multiplying the aerosol volume (within the size range of 10 to 400 nm) by the average mass loading of the wet season (1.4 $\mu g\ m^{-3}$).

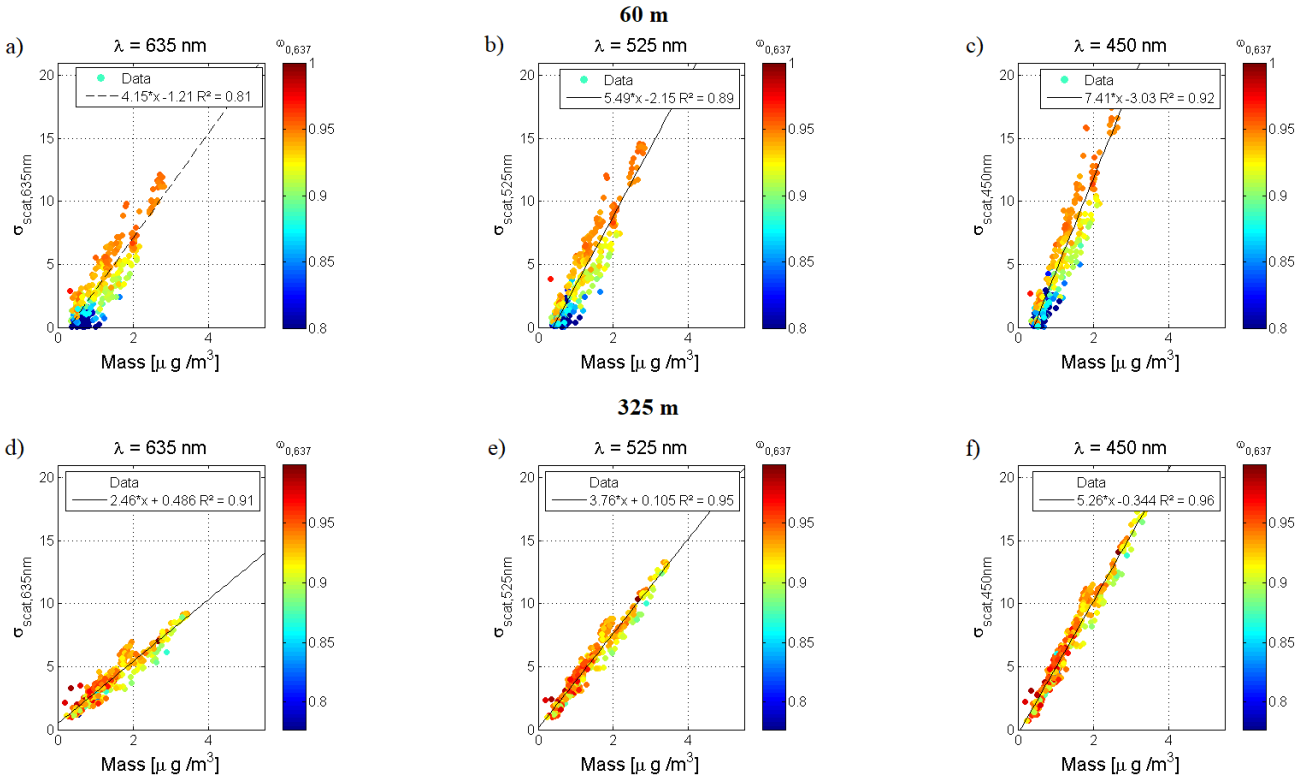

Figure S11. Spectral dependence of the scattering coefficient, σ_{scat}, as a function of mass concentration for measurements at 60 and 325 m height from 8 to 19 May 2019. Panels a), b) and c) represent the scattering coefficient measurements at 60 m height, and panels d), e) and f) represent measurements at 325 m height, at wavelengths of 635, 525, and 450 nm, respectively.

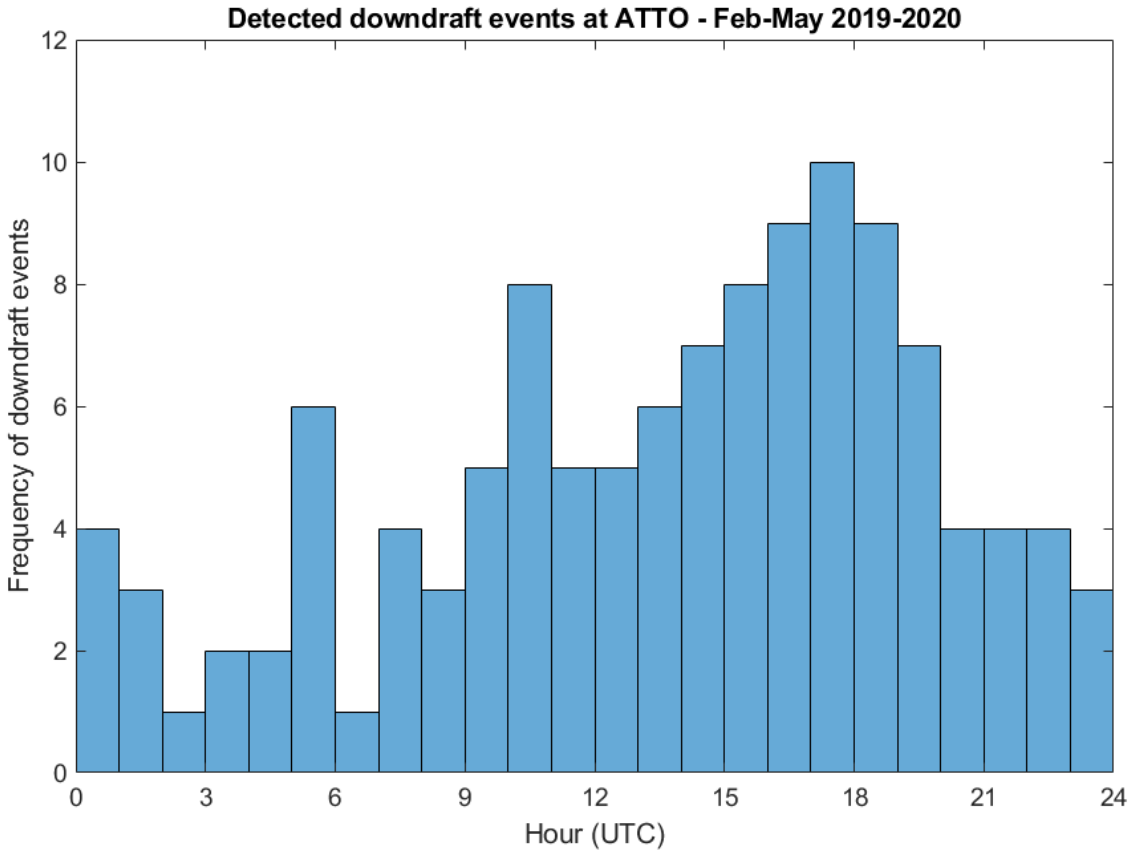

Figure S12. Histogram showing the starting hour of the detected intense downdraft events.

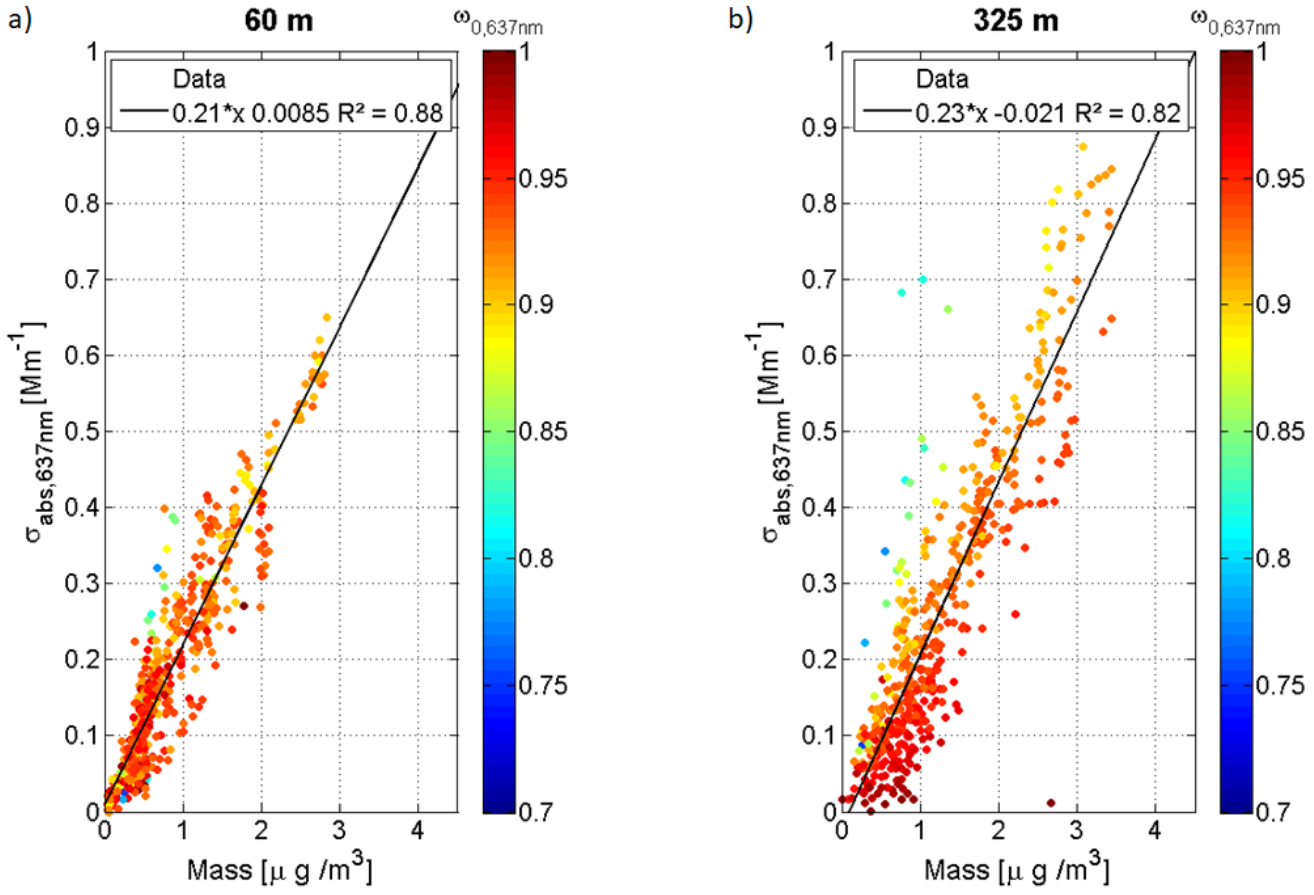

Figure S13. Total absorption coefficient, $\sigma_{abs,637nm}$, as a function of mass concentration for measurements at 60 and 325 m height. Panels a) and b) show the linear fits (black line) and the slopes ($\alpha_{abs,637nm}$) for 60 and 325 m, respectively.

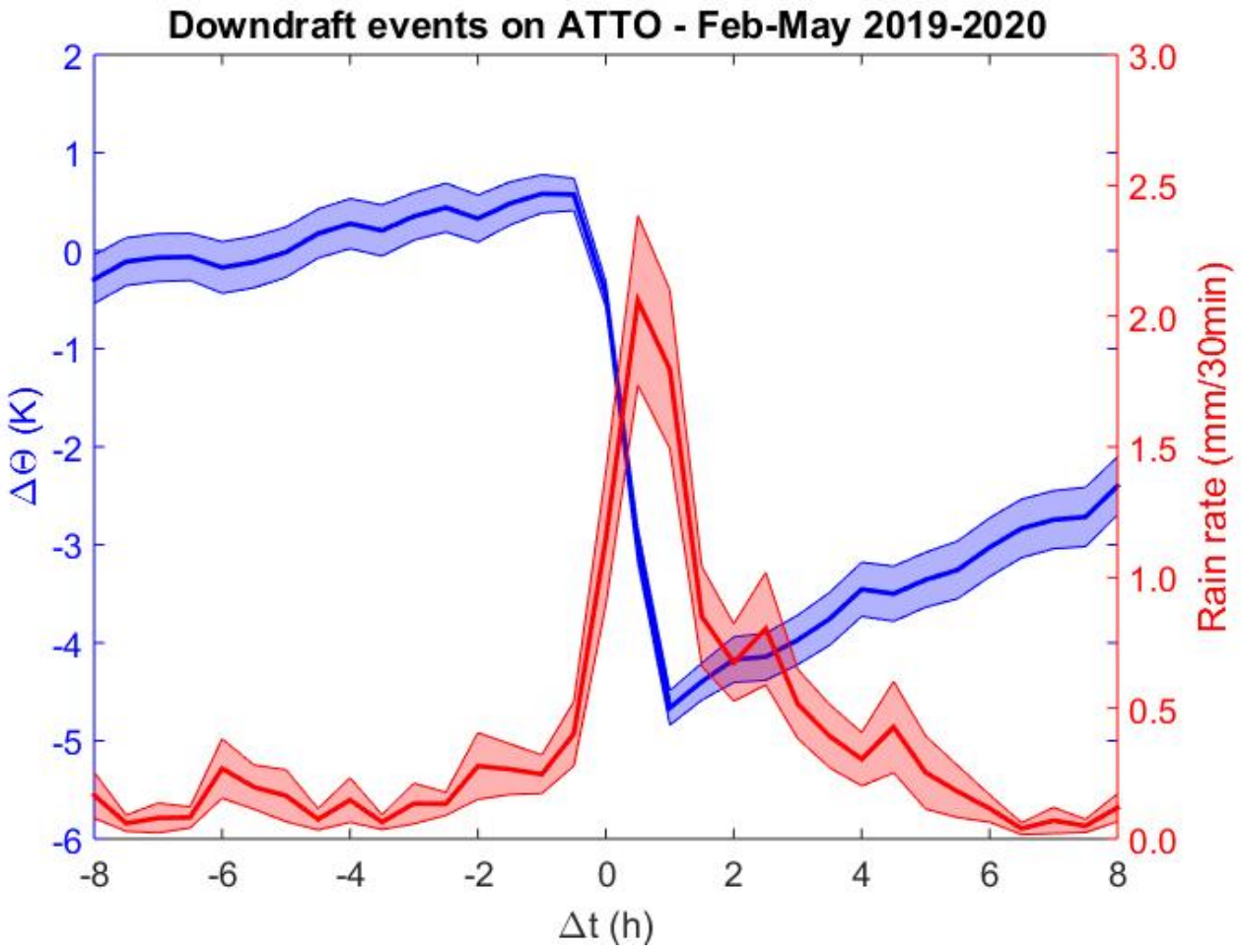

Figure S14. Composite analysis, considering the relative position of the data points to the onset of the closest detected downdraft event, for the potential temperature anomaly (blue) and precipitation rate (red) in a 16-hour window around the onset of downdraft events. The solid lines are the average values and the shaded areas represent the standard deviation of the mean.

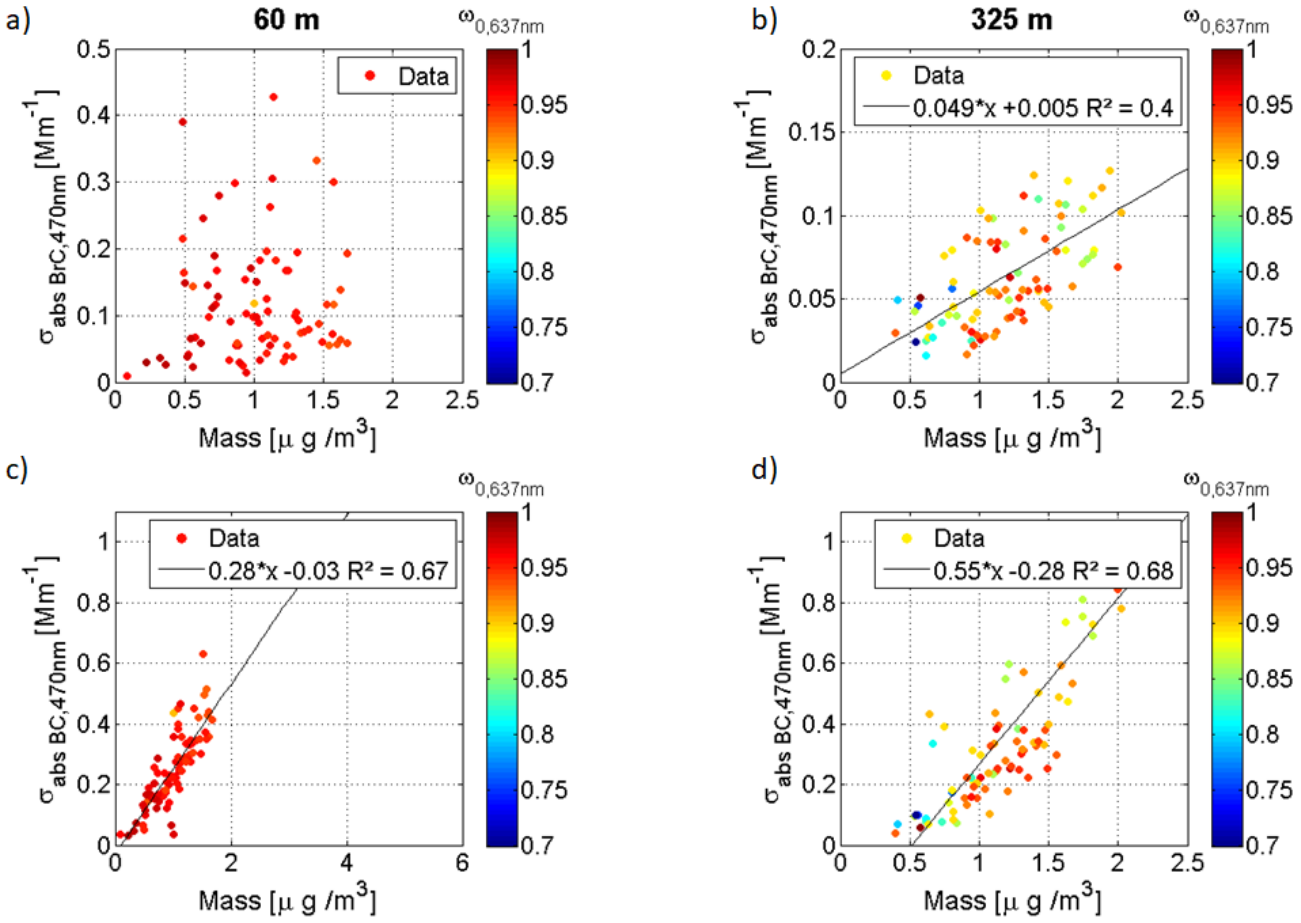

Figure S15. Absorption coefficient, $\sigma_{abs,637nm}$, as a function of mass concentration for measurements at 60 and 325 m height. Panels a) and c) show the linear fits (black line) and the slopes ($\alpha_{abs,637nm}$) for BC and BrC absorption coefficients, respectively, at 60 m height, and panels b) and d) show the linear fits (black line) and the slopes ($\alpha_{abs,637nm}$) for BC and BrC absorption coefficients, respectively, at 325 m height. Please note the different y-axes.